EXPERIMENTS WITH A SUPERSONIC TUBE WIND-TUNNEL

Joseph A. Johnson, III and Dominic Cagliostro
Department of Engineering and Applied Science
Yale University

March 1970

ARNOLD ENGINEERING DEVELOPMENT CENTER

AIR FORCE SYSTEMS COMMAND

ARNOLD AIR FORCE STATION, TENNESSEE

NOTICES

EXPERIMENTS WITH A SUPERSONIC TUBE
WIND-TUNNEL

Joseph A. Johnson, III and Dominic Cagliostro
Department of Engineering and Applied Science
Yale University

FOREWORD

This technical report has been reviewed and is approved.

Carlos Tirres
Captain, USAF
Research Division
Directorate of Plans
   and Technology

Harry L. Maynard
Colonel, USAF
Director of Plans
   and Technology

ABSTRACT

An experimental study has been performed of the unsteady processes in
the starting period of a supersonic Ludwieg tube, a device which operates
like an intermittent supersonic wind tunnel. A quick opening diaphragm lo-
cated downstream of the nozzle initiates the flow. Pressure and density
measurements are made in a variety of ways in Mach number 1.67 and 3.0 noz-
zles. For the starting conditions treated, supersonic flow is established
in the nozzle without producing shock waves. Various time dependent func-
tions are observed in the adjustment of gasdynamic parameters to their steady
supersonic values. These changes of pressure, etc., include undershoots,
overshoots, and other variations of the final steady-state values. Calcula-
tions based on an assumed zero-length nozzle do not adequately predict start-
ing times and pressures.

CONTENTS

ILLUSTRATIONS

NOMENCLATURE

A	area
$\bar{A}$	non-dimensional sound speed
a	sound speed
M	Mach number
P	pressure (atm)
p	pressure
R	gas constant (atm cm^3/g-°K)
R_e	Reynolds number
s	entropy/mass
T	temperature (°K)
t	time (msec)
t_i	total starting time
t_{i1}	time to establish sonic flow in nozzle throat
t_T	total time of stable supersonic flow
U	non-dimensional velocity
u	velocity in x direction
X	distance coordinate (in.)
x	distance coordinate
γ	ratio of specific heats
ρ	density (g/cm^3)
τ	non-dimensional time
z	non-dimensional distance

SUBSCRIPTS

1	initial conditions in low pressure tube

4 initial conditions in high pressure tube

st steady state

I

INTRODUCTION

For vehicles which fly at M > 3 and high altitudes, current testing facilities can simulate Reynolds numbers, Mach numbers and flight environments with adequate success so that flight performance can be predicted from model and full scale experiments (e.g. Ref. 1). However, in the Mach number range 0.8 < M < 3, this is less true. The high Reynolds numbers experienced by aircraft and space vehicles cannot be satisfactorily reproduced in the laboratory. For example, at M ~ 3.5 the Saturn V flies at R_e ~ 2 x 10^6 whereas at M ~ 1.5 the Reynolds number is as high as 10^7 (based on vehicle length). Throughout this Mach number range, testing facilities currently available produce Reynolds numbers of only roughly 2 x 10^6. Since Reynolds number simulation under these circumstances in a crucial aspect of vehicle design, considerable interest has developed in attempts to produce testing facilities with high stagnation pressure, long test time at transonic and moderately supersonic speeds.

Several years ago, H. Ludwieg suggested in a different context a device which now appears to be remarkably well suited for this kind of application (2). The device consisted of a long cylindrical tube as a container for the compressed air. One end of the tube is closed; the other end contained a supersonic nozzle, a test section and a quick opening valve which is opened to the atmosphere. In the Yale University Ludwieg tube (3) a conventional shock tube configuration is modified by the insertion of a supersonic nozzle into the section upstream of the diaphragm (the high pressure section). After the diaphragm breaks a shock wave and a contact surface travel downstream and the head of the expansion wave moves upstream through the supersonic nozzle. After the remaining part of the expansion wave is swept back downstream, stable conditions of supersonic flow are maintained in the nozzle until the reflected expansion wave returns to the throat. The operating stages for this intermittent tube-wind-tunnel (also known as the "Ludwieg tube") are indicated in Figure 1, a t - x diagram with a sketch of the tube. When the diaphragm is ruptured, a centered expansion wave is formed and moves upstream into the high pressure tube where the gas is at the initial conditions denoted by 4. Part of it passes through the nozzle and travels to the end of the high pressure tube where it is reflected and returns to the nozzle. This marks the end of the first steady flow period. When the diaphragm breaks, a shock wave is formed and travels downstream followed by the contact surface into the dump tube where the initial conditions of the gas are denoted by 1. The times shown are t_i, the total starting time; t_{ii}, the time required to establish sonic conditions at the nozzle's throat; and t_T, the total time of stable supersonic flow. In the literature, one can find derivations of the formulas relating the nozzle parameters to the initial conditions in the tube. In these analyses, it is generally assumed that the nozzle has zero length, that the flow is one-dimensional and inviscid and that one is dealing with a perfect gas as shown e.g. by Cable & Cox (4) and Becker (5). With this device, high stagnation pressures can be maintained in the high pressure side and steady supersonic flow of relatively short but useful duration can be established in the test section. Furthermore, a practical advantage with respect to high pressure blow-down tunnels arises from the fact that no valves are required to maintain steady nozzle supply conditions. For these reasons, interest now

1
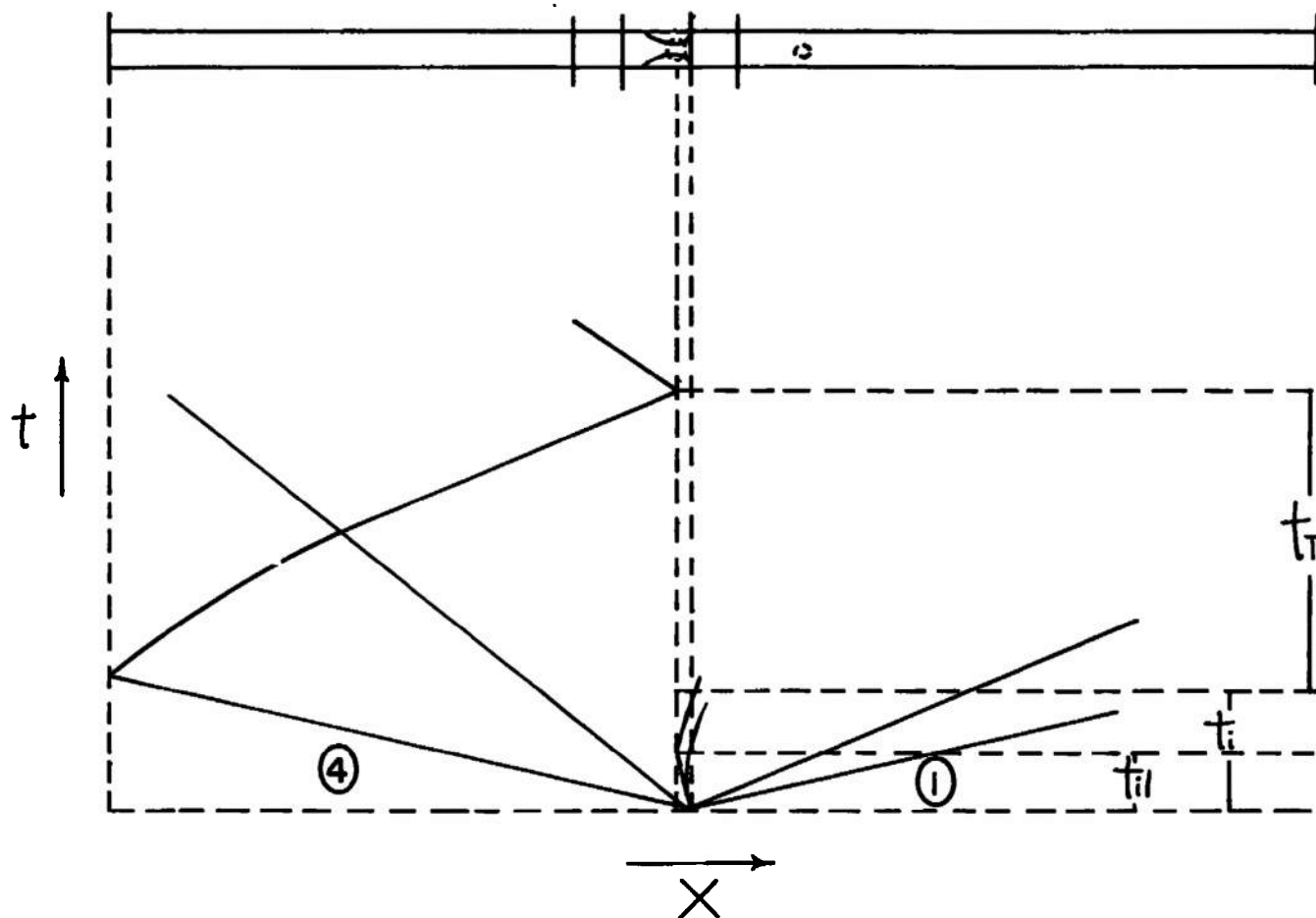
Figure 1 Ludwieg Tube: Simplified t - x plot. The times schematically indicated are t_i, the total starting time; t_{i1}, the time required to establish sonic conditions at the nozzle's throat; t_T, the total time of stable supersonic flow.

exists in the Ludwieg tube and in the nature of its possible application.

With regard to the starting stage, that is, the elapsed time between the rupture of the diaphragm or the opening of a valve and the establishment of steady supersonic flow in the nozzle, some uncertainties have persisted. First, there is the question of whether or not starting shock waves are produced after sonic conditions are obtained at the throat of the nozzle. Such shocks may originate at the throat and travel downstream through the nozzle prior to the steady flow stage and may have adverse effects on the model. In addition, there is the question of how, in fact, the steady state parameters in the nozzle are acquired.

In this paper we shall present further initial results from our observations of starting processes in a supersonic Ludwieg tube*. Our approach has been phenomenological; we are concerned at this point only with experimentally determining what seem to us to be the gross qualitative features of this starting phase. We are interested in observing the sensitivity of the starting processes to changes in nozzle pressure, tube pressure ratio across the unruptured diaphragm, and nozzle Mach number.

---

*Preliminary results have been given in Reference 6.

II

EXPERIMENTAL APPARATUS

The Yale University Ludwieg tube (3) is sketched in Figure 2. The overall length is 26 ft, and a diaphragm can be placed on either side of the test section*. The two dimensional wedge-nozzle used in most of these studies has an exit Mach number of 1.67 and a throat to exit distance of six inches with an expansion half-angle of three degrees. It can be placed at various positions in the 1.5 ft test section so as to vary the field of view. Two sections immediately upstream and downstream of the test section respectively produce a smooth transition from the circular supply and dump tubes to the rectangular test section. In all experiments, the operating gas is dry nitrogen or dry air.

Three diagnostic techniques have been used in our investigations:

(1) Timed shadowgraphs are made during the starting stage. High speed movie shadowgraphs with a 0.25 msec frame to frame sampling rate are taken using a Fastax camera. Spark shadowgraphs are taken at 0.1 msec intervals using a 1 μsec 10,000 volt spark source.

(2) Slit streak-interferometry is used to obtain density measurements as a function of time on the nozzle center-line. A horizontal slit is placed between the light source and the collimating lens so that its image appears at the test section with a width of 2 mm. This, together with the equivalent film speed of 300 m/sec, gives a time resolution of roughly 7 μsec. The Zeiss Mach-Zehnder interferometer** (plate size; 4 1/8" x 7") is adjusted so that the image of vertical interference fringes appears at the center of the test section. With the rotating prism in the Fastax movie camera removed and with the film moving in a vertical plane, continuous interferograms are obtained which allow one to follow the movement of each fringe, thus permitting a determination of the change in density with time at any position along the centerline of the nozzle. Shock waves would be noticeable as discontinuous jumps in the otherwise smooth increase and decrease in density that can be seen according to the direction of motion of the fringes. The system is found to be sensitive to density changes of less than 1.0%.

(3) Static pressure measurements have been made in the supply tube and at various locations in the nozzle using a calibrated high speed 3 μsec rise-time quartz pressure-transducer (Kistler, Model #606L).

For a more detailed description of the tube wind tunnel and auxiliary equipment, see Appendix I.

---

*Downstream diaphragm used in all experiments.

**We are grateful to the U.S. Naval Ordnance Laboratory for loaning us this instrument.
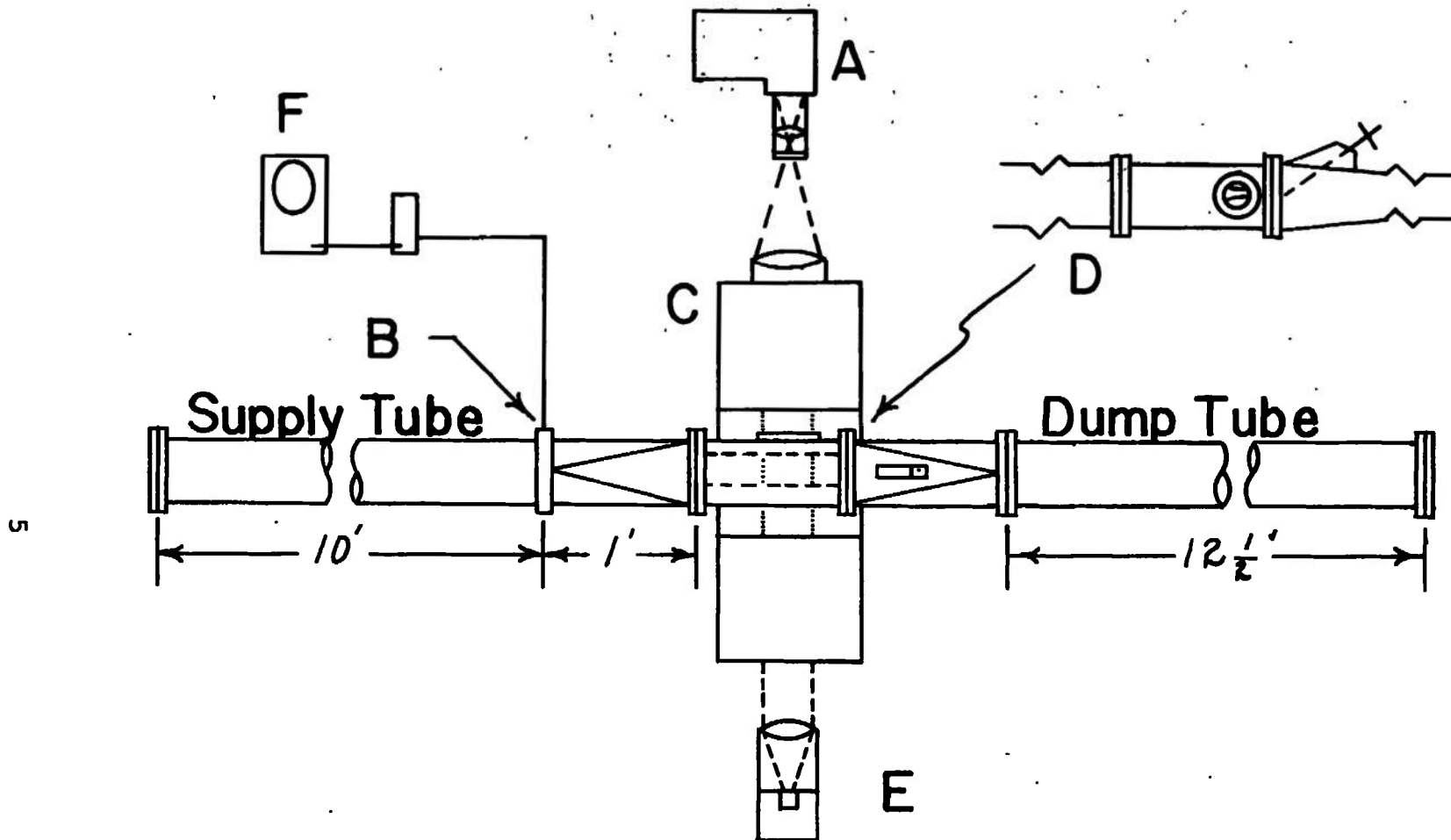
Figure 2 Experimental Apparatus. (A) High Speed Camera. (B) Pressure Transducer (at upstream position). (C) Mach-Zehnder Interferometer. (D) Side View of Test Section. Supply Tube: 5.30 in. I.D. Dump tube: 3.76 in. I. D. Nozzle: 2" x 2" at throat (M = 1.67 at exit). (E) Collimating Lens and Light Source. (F) Oscilloscope to record pressure traces.

III

EXPERIMENTAL RESULTS

Spark shadowgraph pictures are taken during steady flow with a model inserted in the test section producing bow shock waves to confirm that supersonic flow is established (see Appendix II). Movie shadowgraphs are taken with fiducial marks on the test section window and with adhesive strips along the diverging section of the nozzle and perpendicular to the flow. The relative position of the disturbances from the adhesive strips with the marks on the window indicates when supersonic flow begins and reaches steady state. Finally, movie shadowgraphs and spark shadowgraphs of the flow in the nozzle permit a search to be made for starting shocks in the starting stage. Table I lists the operating pressures for the experiments with movie shadowgraphs. When more than one movie is indicated, this means that different regions in the nozzle have been sampled or that models have been inserted into the test section. In addition, a set of spark shadowgraphs has been taken during the starting stage for $P_4 = 1.0$ atm and $P_4/P_1 = 7.7$ with a sampling rate of better than one every 0.1 msec.

In none of these experiments have starting shock waves been observed. This is illustrated in Figure 3 where $P_4 = 3.0$ atm and $P_4/P_1 = 23$ for the $M = 1.67$ nozzle. Here one sees supersonic flow being established in the nozzle with no waves other than the disturbances from the adhesive strips on the nozzle block. The supersonic flow appears to develop smoothly at all points in the nozzle. Similar results are obtained for all cases studied by us. In Figure 4, one sees an example of the movie interferogram by which one can look for starting shocks with even greater reliability. Furthermore, density histories at fixed nozzle position and density profiles at specific times in the starting stage can be determined. The experiments during which movie interferograms were made are also indicated in Table I. The range of upstream pressures and of pressure ratios is nearly the same as that for the movie shadowgraphs. In Table I one sees that neither the interferograms nor the shadowgraphs show starting shocks. With a total of seventeen experiments performed, including five experiments at $P_4 = 3.0$ atm and $P_4/P_1 = 46$, one finds no indication in these data of a starting shock prior to the establishment of supersonic flow.

Examples of density measurements are given in Figure 5. The throat of the nozzle is at $X = 0$ and the time scale is arbitrarily chosen so that $t = 0$ corresponds to the first appearance of the head of the expansion fan roughly 3.5 in. downstream of the throat. One can see the density drop to values that are at first below those of its final steady state. This "undershoot" is about 4% at $X = 0$; however, its magnitude decreases with increasing downstream distance. One also notices that the undershoot occurs in about 2 msec at the throat and that it precedes the appearance of an undershoot at the downstream distance for $X > 0$. Density profiles are also shown in Figure 5 for this case of $P_4 = 3.0$ atm and $P_1 = 0.40$ atm. At all times, the densities show a decrease with increasing downstream distance. Here, as before, there is no indication of starting shock waves. Comparisons of the density measurements in Figure 5 with density measurements at other values of P_4 (with $P_4/P_1 = 7.7 =$ const.) have given the following results: The values

Table I. Summary of Experiments M = 1.67

P_4 (atm)	P_4/P_1	No. of Movie-Shadowgraphs	No. of Movie-Interferograms	Starting Shocks Formed?
3.0	46	3	2	No
3.0	23	1	----	No
3.0	12	1	----	No
3.0	7.7	2	2	No
3.7	7.7	----	1	No
2.0	7.7	----	1	No
1.0	7.7	3	1	No

$t = t_o$ $t = t_o + .2$ msec $t = t_o + .4$ msec

$t = t_o + .6$ msec $t = t_o + 1.0$ msec $t = t_o + 1.2$ msec

$t = t_o + 1.4$ msec $t = t_o + 1.6$ msec $t = t_o + 1.8$ msec

$t = t_o + 2.0$ msec $t = t_o + 2.4$ msec $t = t_o + 3.0$ msec
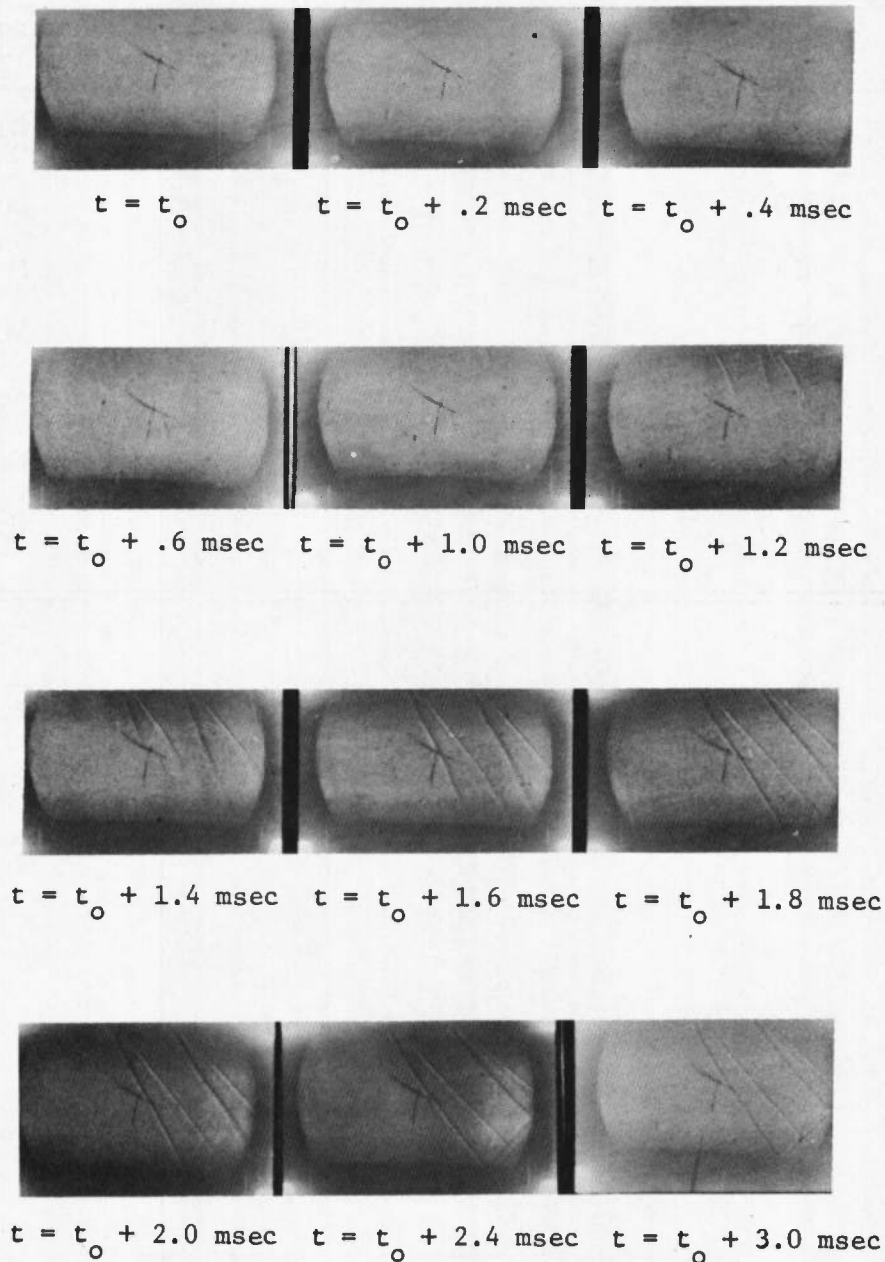
Figure 3   Sequential Shadowgraphs in Starting Stage. Shock waves are produced by an adhesive strip taped to the top of the M = 1.67 nozzle.
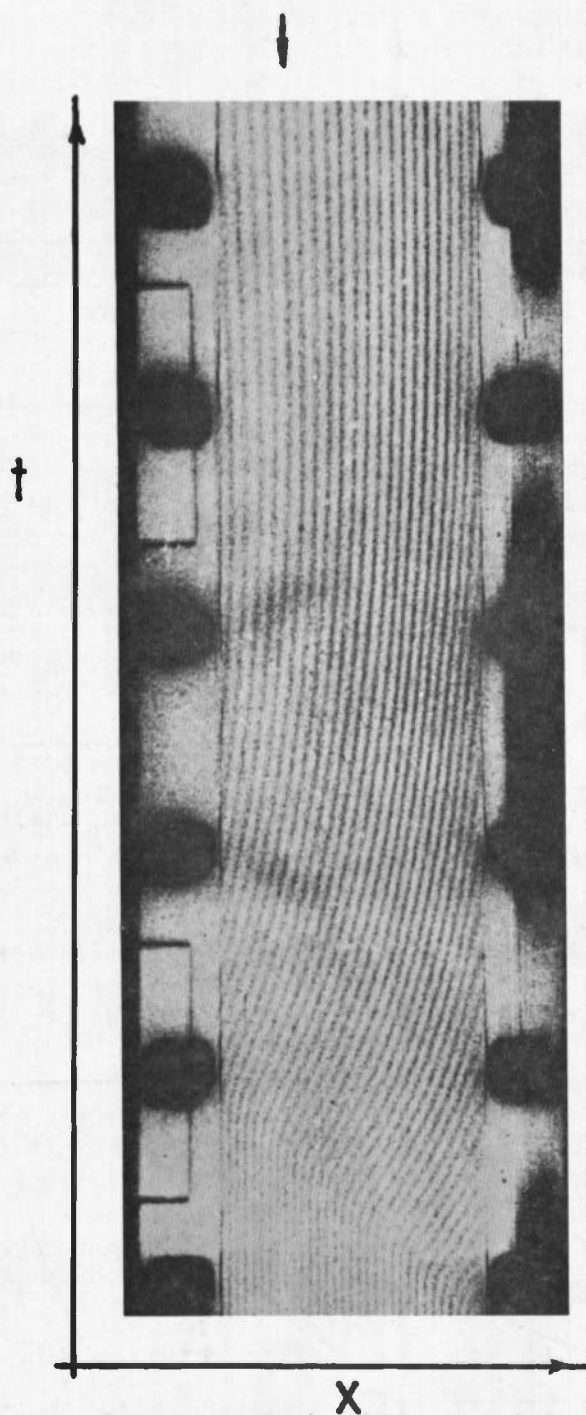
Figure 4 Sample Interferometer Strip. The M = 3.0 nozzle's throat is indicated by the arrow. Decreasing densities are indicated by the motion of fringes from left to right. Flow is from left to right.

9

$$P_4 = 3.0 \, atm; \, P_4/P_1 = 7.7; \, M = 1.67$$
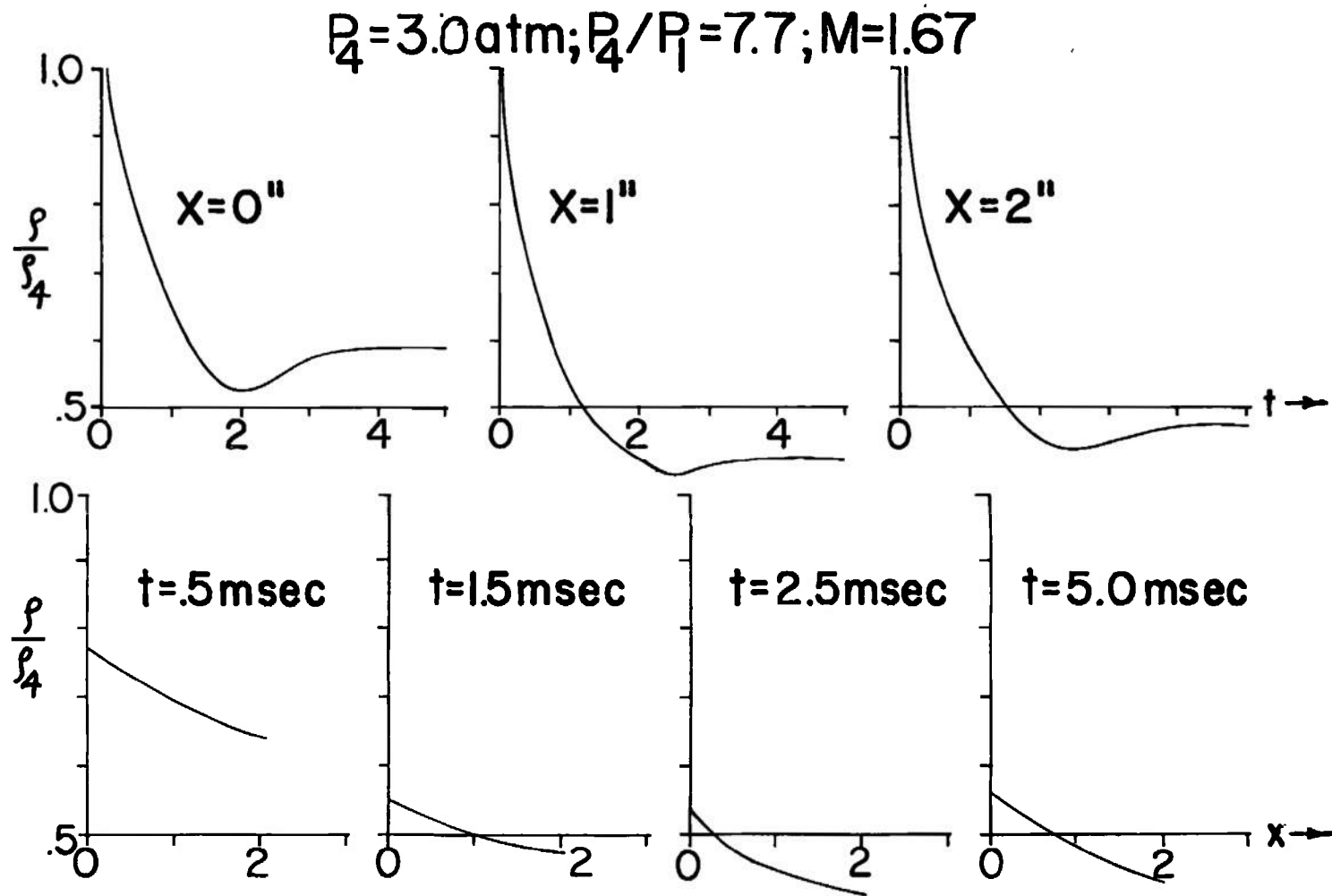
Figure 5   Sample of Density Measurements.   Distances are measured in inches from the throat of the nozzle.   Times are measured in milliseconds, with t = 0 corresponding to first appearance of the expansion fan roughly 3.5 in. downstream of the throat.

of ρ/ρ_4 obtained at the throat are independent of P_4; hence the percentage undershoot is also independent of P_4. The undershoot times are independent of P_4. Further, the density profiles always show a monotonic decrease with increasing downstream distance. Generally, we have found that the data in Figure 5 are representative of all density measurements performed.

Direct measurements of static pressure histories in the nozzle provide additional checks on the existence or absence of starting shock waves. In addition, comparisons can be made with the density histories mentioned above. Pressure as a function of time at three different locations in the $M = 1.67$ nozzle is given in Figure 6. The starting point of the time scale is arbitrary. At $X = 0$ in. the pressure drops initially below its final value while at $X = 5.2$ in. this undershoot is considerably diminished; outside the nozzle at $X = 6.3$ in. this behavior has practically disappeared. These results are consistent with the density measurements shown in Figure 5 where the relative undershoot also decreases with increasing downstream distance. Density measurements made at the nozzle's exit show the same qualitative trends as the pressure measurements in Figure 6. Finally, Figure 6 provides additional evidence for the smoothness and shock-free nature of the establishment of supersonic flow in the nozzle.

Measurements of static pressure histories in the stagnation region have been obtained for all the experiments given in Table I. Samples of these results are given in Figure 7 for the $M = 1.67$ nozzle*. An undershoot of the steady state values is also seen as a persistent feature. In addition, one finds that the undershoot seems to be followed by an "overshoot" as the adjustment to steady flow values is taking place. By comparing the two results for $P_4 = 3.0$ atm and different P_1 values, one can see that P_1, the initial downstream tube pressure, is not the determining factor as far as the pressure history is concerned, once P_1 is low enough to provide a sufficient pressure ratio for supersonic flow to be established. Changes in P_4 do cause changes in the magnitude of the pressure shifts during starting. However, the times required for the pressure to drop below its final values seem to be independent of both P_4 and P_4/P_1 within the limits stated.

For purposes of comparison, static pressure measurements have also been made in the stagnation region of a two dimensional Mach number 3.0 nozzle. Samples of the data obtained are given in Figure 8. Qualitatively, the results are similar to those observed at the lower Mach number.

For a more detailed description of the experiments and further examples of the results, see Appendix II.

---

*Static and stagnation pressure measurements in the stagnation region are also reported in References 7 and 3. However, these experiments were designed to determine steady state values and gave little information on the starting processes.
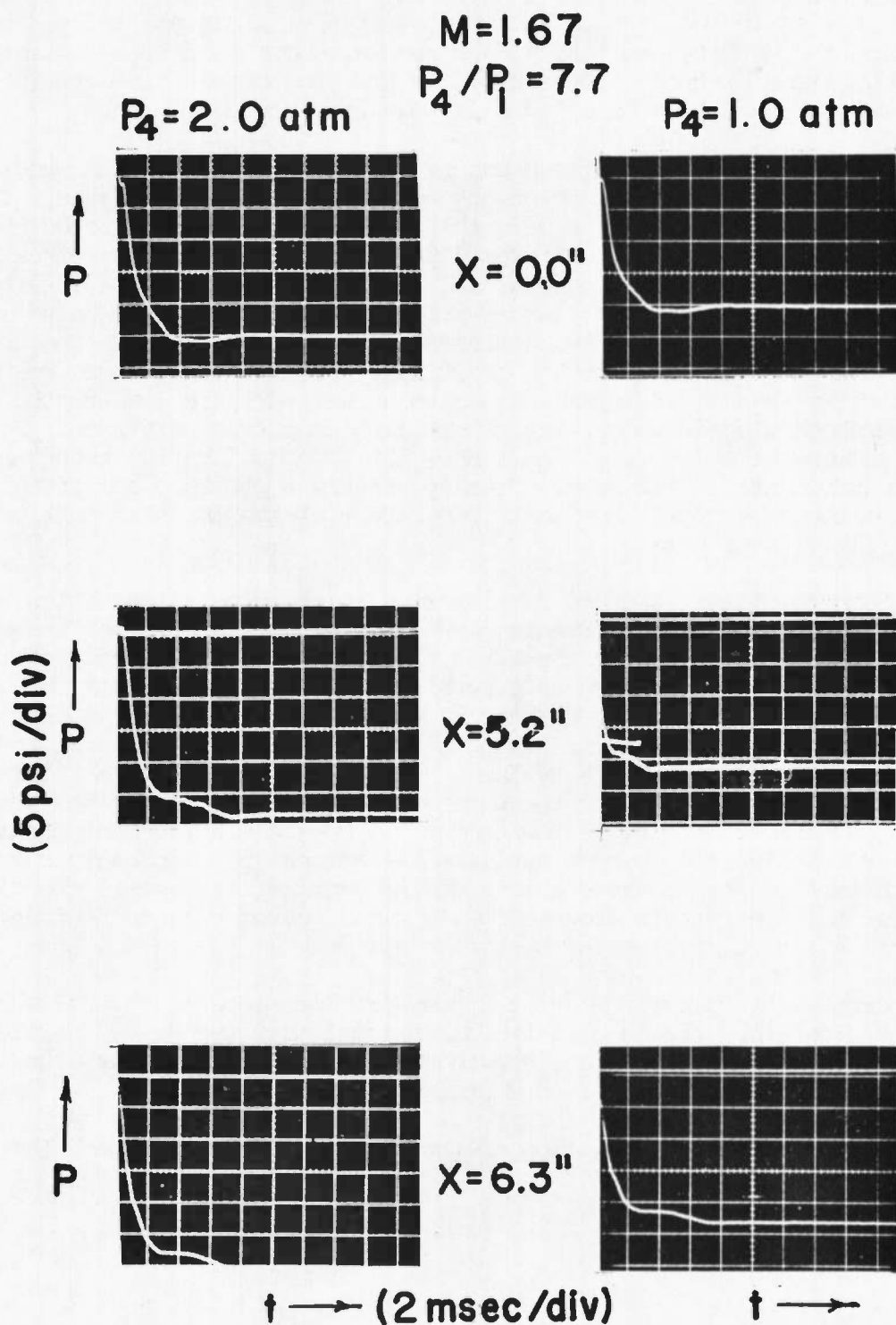
Figure 6   Static Pressure Measurements in the M = 1.67 Nozzle.   The
pressure gauge is being self-triggered in these measure-
ments; the signal required for triggering corresponds to a
pressure change of roughly two psi.

12
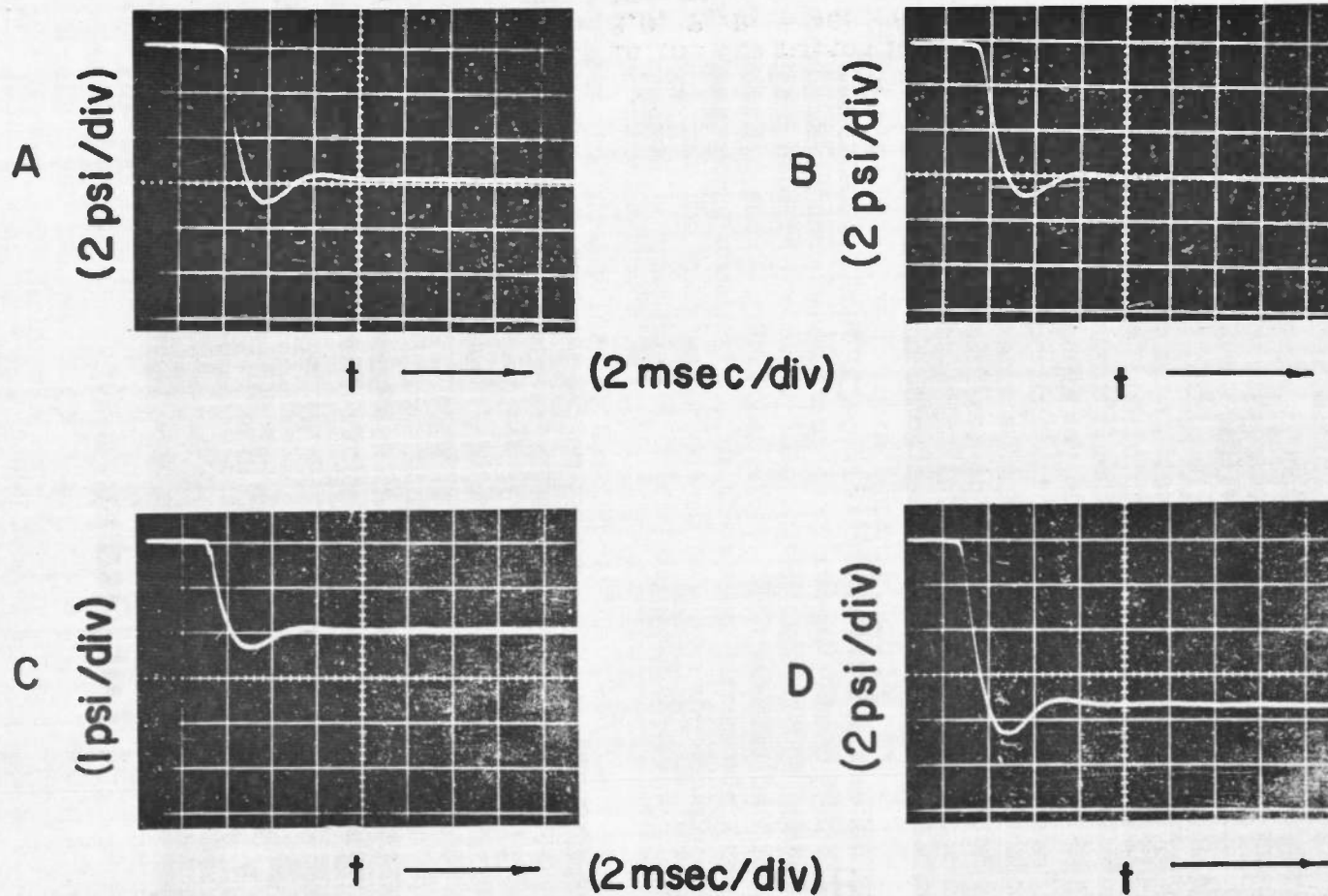
M = 1.67

Figure 7 Pressure Measurements in the Stagnation Region: M = 1.67. (A) $P_4 = 3.0$,
$P_4/P_1 = 7.7$; (B) $P_4 = 3.0$, $P_4/P_1 = 46$; (C) $P_4 = 1.0$, $P_4/P_1 = 7.7$;
(D) $P_4 = 3.7$, $P_4/P_1 = 7.7$. The time scale is arbitrary; the pressure
trace is triggered by a firing pin contact subsequent to the rupture of
the diaphragm. P_4 is in atmospheres.

M=3.0

A   t (2 msec/div) →

B   t (2 msec/div) →

C   t (2 msec/div) →

D   t (1 msec/div) →

(1 psi/div)   (1 psi/div)
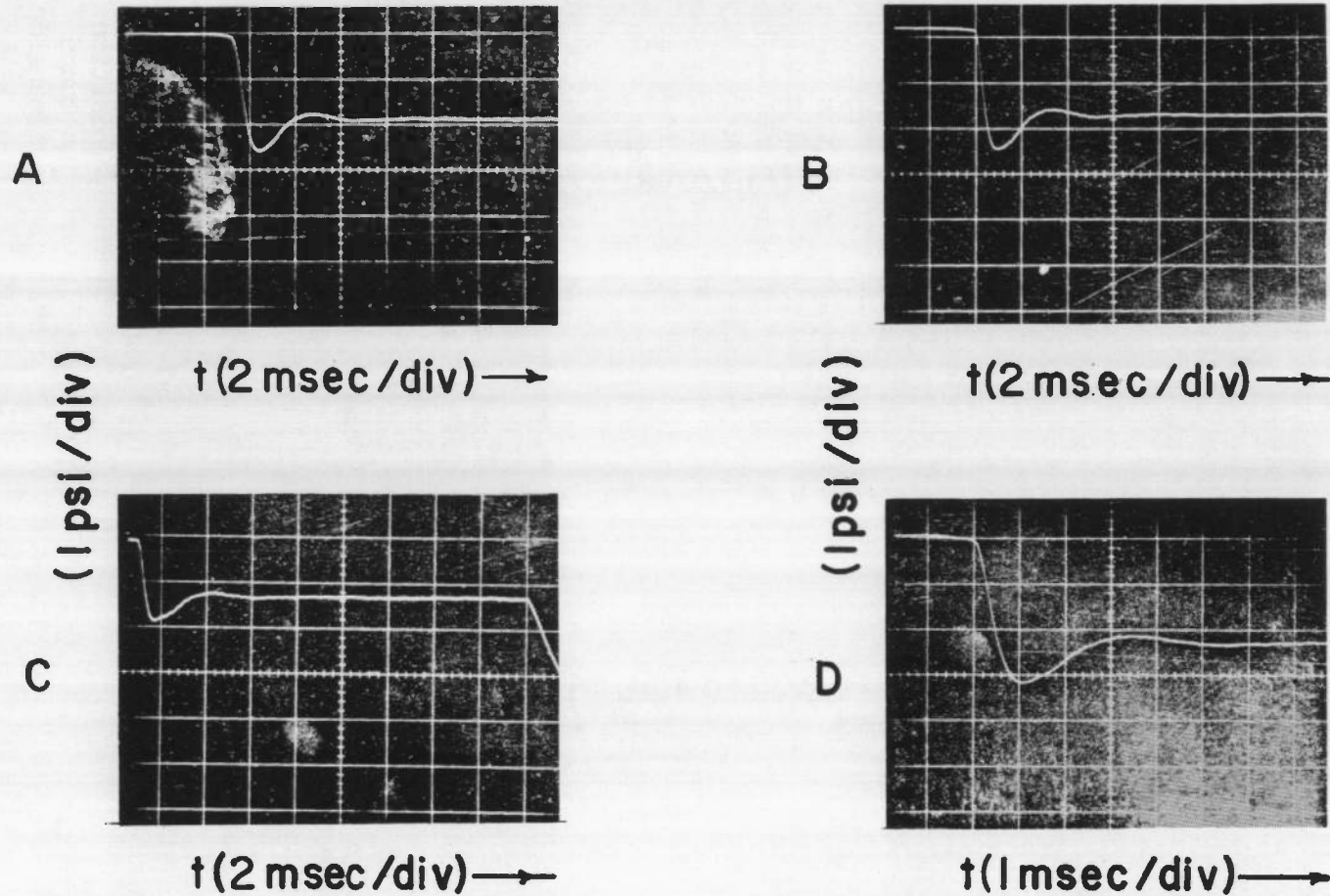
Figure 8   Pressure Measurements in the Stagnation Region: $M = 3.0$.   (A) $P_4 = 3.0$, $P_4/P_1 = 18$;   (B) $P_4 = 3.0$, $P_4/P_1 = 46$;   (C) $P_4 = 2.0$, $P_4/P_1 = 18$; (D) $P_4 = 3.7$, $P_4/P_1 = 18$.   The pressure gauge triggering here is the same as in Figure 7. P_4 is in atmospheres.

IV

DISCUSSION OF RESULTS

For the flow conditions of this work, it has been shown that starting shock waves analogous to those which ordinarily appear in a conventional blowdown wind tunnel are not produced. The absence of starting shocks is important because it reduces the transient forces on a model during tunnel starting and thereby decreases the chance of model breakage and lowers the design requirements of the model and its support. The M = 1.67 nozzle used in this work is a wedge type nozzle with a 6 in. radius arc at the throat and a straight 3° half-angle diverging section and the M = 3.0 nozzle is a continuously expanding nozzle with a cubic profile, as compared to nozzles designed by using the method of characteristics which produce parallel supersonic flow at the exit. This nozzle design may effect the results. We recall that the diaphragms used in these experiments require less than 0.1 msec to burst. By contrast roughly 1 msec is required for the head of the expansion wave to traverse the nozzle. This time is called the characteristic nozzle time. Thus, the diaphragm rupturing process is fast relative to the characteristic nozzle time. On the other hand, the valve opening process in a blowdown wind tunnel is typically slow relative to characteristic nozzle times. It is therefore possible that a Ludwieg tube using slow opening diaphragms or valves and a short nozzle would produce starting shock waves. For the M = 1.67 nozzle, boundary layer effects are negligible in the experiments using supply pressures between 1.0 and 3.7 atmospheres(5). This conclusion follows from the density measurements obtained during the steady supersonic flow in the nozzle. It was found that the Mach number determined from the density ratio was practically equal to that predicted from the geometrical area ratio.

However, the theory for the Ludwieg tube's operating parameters for zero nozzle length (e.g. Reference 4) is not entirely adequate. For example, it predicts for M = 1.67 that the steady state static pressure should be 86% of the supply pressure $(P_{st}/P_4 = 0.86)$ while the measured result is $P_{st}/P_4 = 0.83 \pm .01$. The predicted duration of the steady flow at the stagnation regions pressure station is 17 msec. The corresponding measured time between the appearance of the head of expansion wave and its reflection which terminates the steady flow agrees with the prediction. However, due to the starting process whose duration varies from 5 to 7 msec (depending on P_4), the actual time of steady flow is only about 12 msec.

It was found that we could make some correct predictions by using a simplified one-dimensional treatment (see Appendix III). In these calculations, we use the method of characteristics applied to our tube configuration for unsteady one-dimensional flow in the M = 1.67 nozzle. It was assumed that the flow was initiated by an expansion fan at the diaphragm position. The gas was again assumed to be perfect and inviscid. It was then found theoretically that 1.6 msec after the arrival of the head of the expansion wave at the throat of the nozzle, the density at the throat (X = 0) is $\rho/\rho_4 = 0.51$. This can be compared with the measured undershoot time and density of t = 1.9 msec and $\rho/\rho_4 = 0.52$ respectively. Both theory and experiment give the steady state values $\rho/\rho_4 = 0.57$ and therefore the initially lower density value is verified theoretically.

In Figure 9, finally, two quantitative aspects of the undershoot in the static pressure measurements in the stagnation region are shown. First of all, it is suggested in our data that the ratio of minimum pressure to the steady state pressure is independent of the upstream starting pressure. For a given nozzle, we show in Figure 9 data at a single fixed pressure ratio. However, the measurements at pressure ratios of 46, 23, and 12 for M = 1.67 and of 46 for M = 3.0 show these results to be indeed independent of pressure ratio. Secondly, the experiments suggest that the undershoot time and the overshoot time are independent of the starting pressure. This is also shown in Figure 9. The time between the onset and the termination of the expansion phase in the stagnation region is observed to be insensitive to changes in the upstream supply pressure. Nonetheless, the total starting time, not shown in these presentations, does seem to be sensitive to P_4.

$$R = \frac{|P_D - P_S|}{P_4}$$

$$F = |P_S| / P_4$$

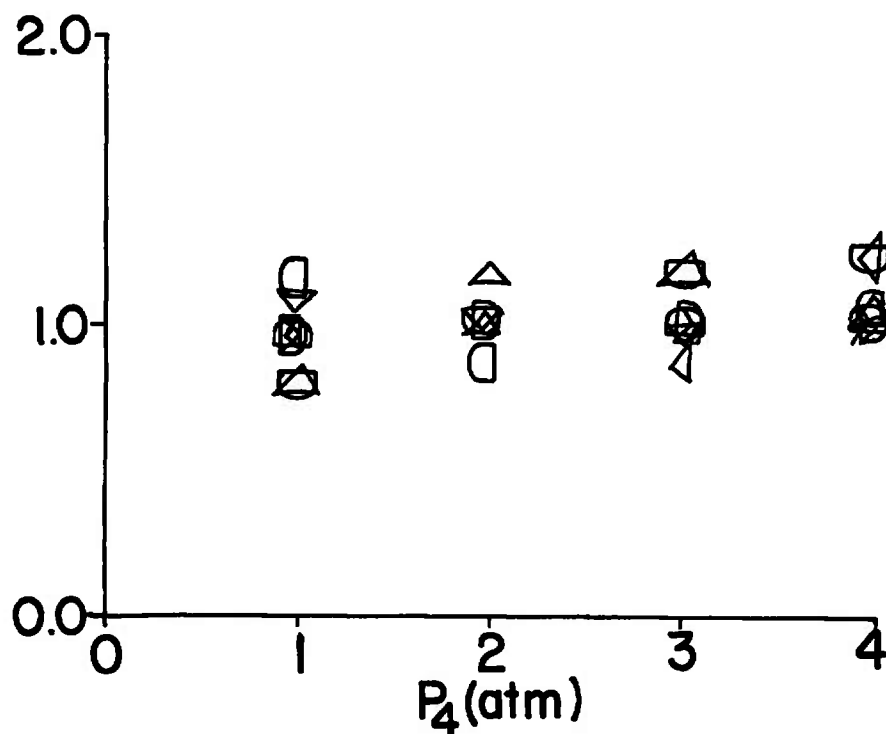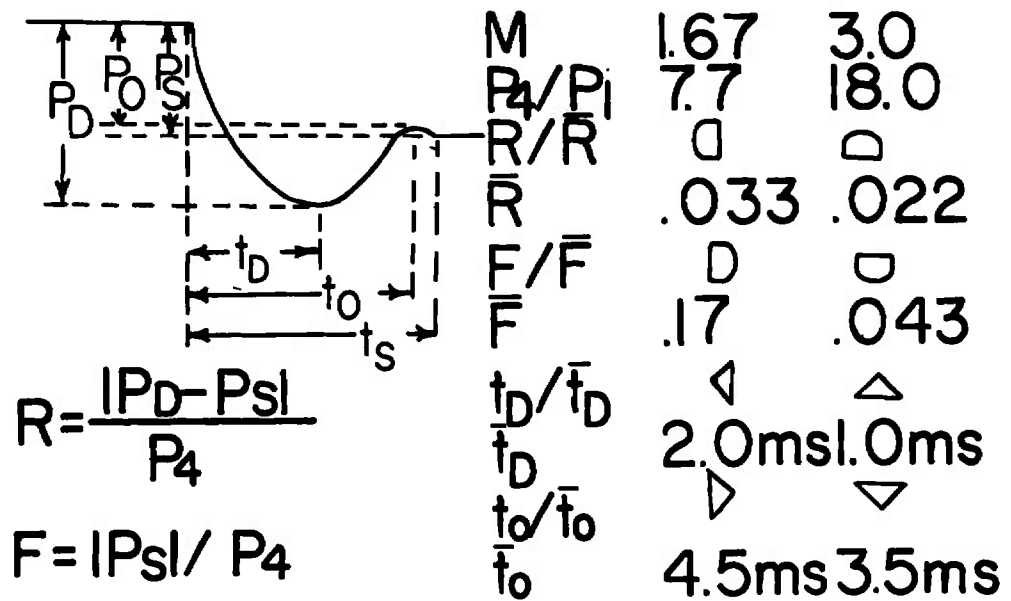|		
M	1.67	3.0
P_4/P_i	7.7	18.0
$R/\bar{R}$	◖	◗
$\bar{R}$	.033	.022
$F/\bar{F}$	◖	◗
$\bar{F}$	.17	.043
$t_D/\bar{t}_D$	◁	△
t_D	2.0ms	1.0ms
$t_o/\bar{t}_o$	▷	▽
t_o	4.5ms	3.5ms

Figure 9   Starting Times and Pressures in the Stagnation Region: Insensitivity to P_4.

17

V

SUMMARY

From our experimental and theoretical studies of the starting processes for the Ludwieg tube wind-tunnel with two nozzles of $M = 1.67$ and $M = 3.0$ respectively, for the range of conditions treated in our experiments, we find: (1) Steady supersonic flow can be established smoothly throughout our type of continuously diverging nozzle past the throat, without the formation of starting shock waves. When sonic conditions have moved to the throat of the nozzle, supersonic flow has already begun in the downstream portion of the nozzle. These results appear to be independent of the supply pressure P_4 and of the starting pressure ratio P_4/P_1, once this ratio is sufficiently large to produce supersonic flow. (2) Static pressures and densities are found to first undershoot then adjust to their steady supersonic flow values. The values of the pressure and density drop below the final values decrease with increasing distance from the nozzle's throat. For a fixed Mach number the ratios of minimum pressure and density to supply tube pressure and density respectively and the ratios of time to minimum pressure to the total starting time are independent of P_4 and P_4/P_1. (3) For fixed nozzle Mach numbers, the ratios of steady state pressure to supply tube pressure are independent of P_4 and P_4/P_1. However, the total starting time is found to be dependent on P_4 but not on P_4/P_1. (4) A change in nozzle Mach number changes undershoot and steady state pressures, densities and time.

These results suggest that the deleterious effects arising from the interaction of starting shock waves with test models can be avoided in Ludwieg tube wind-tunnels where use is made of fast opening diaphragms or valves. The observed variations in pressures and densities indicate important inadequacies in a simplified one-dimensional treatment of the gas dynamic processes and show that more sophisticated theoretical techniques are needed if correct predictions concerning the starting stage phenomena are to be obtained.

APPENDIX I

DETAILED DESCRIPTION OF LUDWIEG TUBE WIND TUNNEL

AND AUXILIARY EQUIPMENT

A detailed side view of the tunnel is shown in Figure I-1. The overall length of the intermittent tunnel is 26 ft. and it is fabricated entirely out of stainless steel 304. The high pressure end of the tunnel is made from a 10 ft. length of seamless tube with 5.295 in. I.D. and 0.134 in. wall thickness. A transition piece made out of 1/8 in. plate and 1 ft. in length connects the tube to a rectangular nozzle section 1-1/2 ft. in length and contains a diaphragm rupturing pin. The high pressure end of the tunnel and the transition piece are mounted on linear ball bushings which make it possible by a simple hand push to move the entire tube and transition piece 4 in. away from the nozzle section along the tunnel centerline. This permits insertion and removal of diaphragms for experiments with upstream diaphragm location. Screens may be introduced at this point. The nozzle section follows and will be described in greater detail below. For experiments with diaphragm downstream of nozzle and test section the diaphragm is placed between the nozzle section and another 1 ft. transition section which contains the diaphragm rupturing pin and connects the nozzle section to the low pressure or dump tube. The dump tube is made of seamless tube 3.760 in. I.D. and 0.120 in. wall thickness and consists of two sections. The first section is 2-1/2 ft. long and is connected to the transition piece. The other section is 10 ft. in length. A 2 in. thick insert, the size of a 4 in. pipe flange, is located between these two pipes. The insert contains two quartz windows, 3/4 in. diameter and 1 in. thick, and permits a beam of light to pass through the tube. This arrangement acts as a shock detection station and can be used to trigger the electronic instrumentation. The individual sections of the tube are sealed together by inserts containing O-rings placed between the flanges.

The downstream transition section and dump tube assembly are mounted on linear ball bushings which make it possible to move the entire assemble approximately 1 ft. away from the nozzle section along the tunnel centerline. This permits easy access to the test section as well as insertion and removal of diaphragms. The nozzle section, diaphragm and downstream transition section are held together by a wedge-shape clamping device. The clamping device permits quick connection and disconnection of the two parts of the tunnel.

The entire tunnel assembly is mounted on a 4 in. I-beam and supported by several 4 in. diameter pipes. This arrangement is rigid and permits easy access to any part of the tube. A 3 ft. piece of the supporting I-beam for the test section is removable. The nozzle section and this portion of the I-beam may be lifted and the Mach-Zehnder interferometer (plate size; 4 1/8" x 7"), manufactured by Zeiss Company, positioned in place.

The nozzle section is rectangular with 2 in. by 5 in. inside dimensions and 1-1/2 ft. in length. This section contains the nozzle blocks, test section and model support. The side walls extend to practically the entire length of the section and are sealed to it by means of O-rings. The nozzle blocks are 2 in. in width and rest on the top and bottom of the rectangular
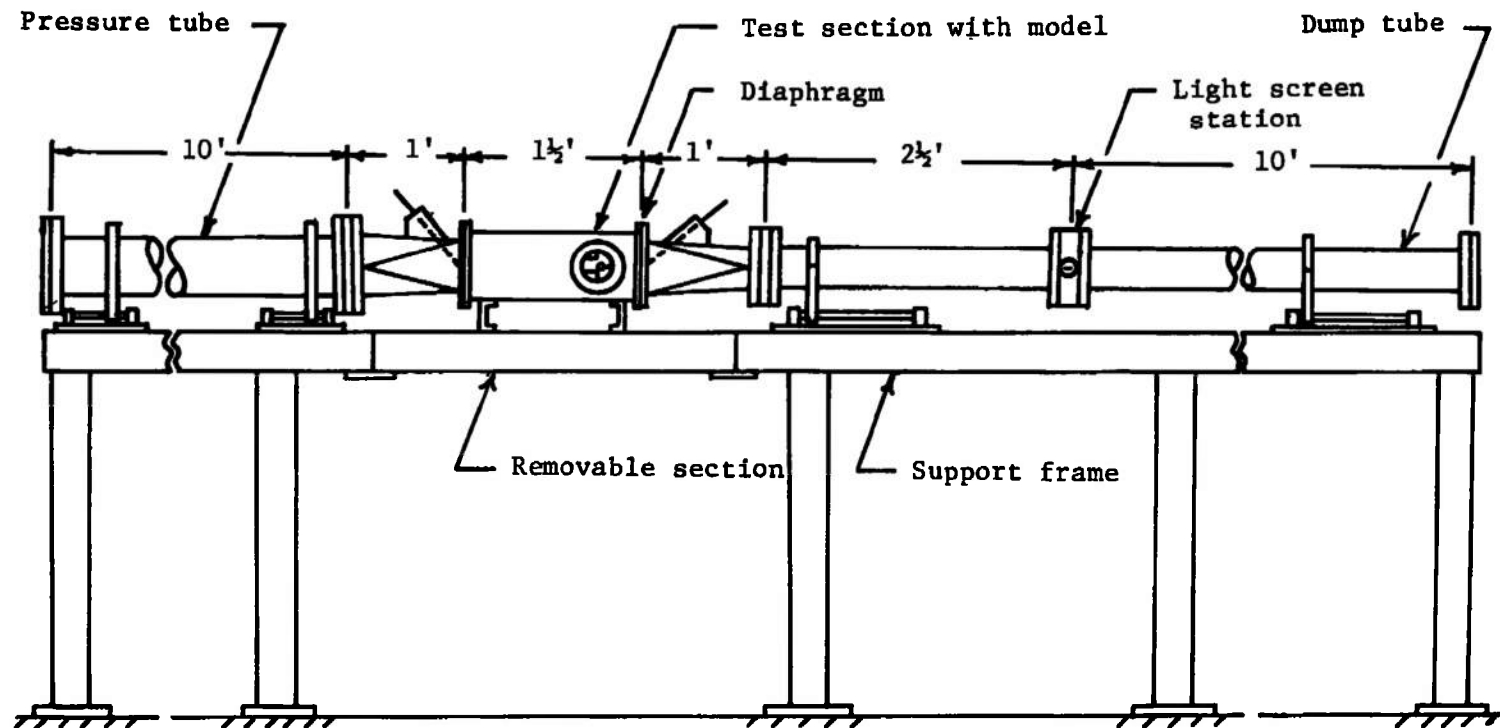
Pressure tube: 5.295 in. I.D., 0.134 in. wall, stainless steel 304 seamless tube.
Dump tube: 3.760 in. I.D., 0.120 in. wall, stainless steel 304 seamless tube.
Nozzle: two dimensional, 2 x 2 in. throat.

Figure I.1   Sketch of the intermittent tube wind tunnel

nozzle section. They are held in place by screws and are sealed by O-rings concentric with the screws. The side walls may be easily removed to exchange the nozzle blocks which have been machined out of Plexiglass. The windows are mounted and sealed in metal frames which in turn are sealed by means of O-rings into the side walls. Windows are held flush with the inside of the nozzle walls by threaded retaining rings. The windows are 4 in. diameter, 1 in. thick, and made of Schott BK-7 glass ground to 1/8 wave length with a wedge angle no greater than 20 min. The location of the windows is 5 in. upstream from the diaphragm. The model support is mounted in the nozzle section near the diaphragm. Models extend into the nozzle section, as viewed through the window, and are easily changed by reaching into the test section while the diaphragm is being changed. For a more detailed description of the equipment see Reference 3.

Instrumentation of the Tunnel

The tunnel is instrumented with a pressure measuring system, a photographic system, a Mach-Zehnder Interferometer, and a supporting electronic system. See Figure 2.

Transient pressure recordings are made with a piezo-electric quartz-crystal pressure transducer (Kistler Model 606L). The transducer may be mounted in an insert between the pressure tube and the upstream transition section, at the pressure tube end plate, and also in the nozzle side wall. The side wall location is 5.5 in. upstream from the diaphragm and the transducer is mounted in a blank which replaces the window when pressure readings are taken. The output of the transducer is amplified by a Kistler Universal Dial-Gain Charge Amplifier Model 504 and it is recorded on an oscilloscope. The rise time is given to be 3 microseconds. Simultaneous pressure recordings at two different locations are obtained by using two pressure transducers and amplifiers. Pressure recordings are made along the nozzle centerline at five positions each 3/4 in. apart by using a special mounting plate in the nozzle side wall.

The Mach-Zehnder Interferometer is located at the test section and is used for density measurements. This is done by streak and still interferograms. It may also be modified so that shadowgraph pictures can be taken. This is done by using the parallel light from the top light path and blocking the bottom light path at the compensation chamber. The same optics and light sources are used. Two light sources, a 100 watt continuous mercury arc lamp with a d.c. power supply and a spark source, can be mounted on the interferometer together with the appropriate lens systems. The continuous light source is used for streak interferograms and high-speed shadowgraph movies while the spark light source is used for still interferograms and shadowgraph pictures.

The flow field in the nozzle is recorded by shadowgraph methods in parallel light which is collimated by means of a f/6, 610 mm focal length Bausch & Lomb Aero Tessar aerial camera lens. A spark light source with a 0.08 cm diameter source is located at the focal point of the lens. The spark source unit has a duration of 0.5×10^{-6} sec. and is of the type suggested by Kovasznay*. A detailed description of the spark source and its power supply

*Kovasznay, L. S. G. 1949 High power short duration spark discharge. Rev. of Sci. Inst. 20, 696.

used here may be found in Klikoff*.

The spark source is triggered by either one of two methods, a light screen shock detection station or a contact on the diaphragm plunger. The first method works in the following manner. After rupture of the diaphragm, the shock wave travels into the dump tube and triggers the light screen by bending a light beam into a phototube. The output of the light screen is then fed into a time delay unit (General Radio Time Delay Generator, Type 1392-A) which in turn triggers a thyratron amplifier and spark source combination after any desired time interval. A detailed description of the light screen arrangement and signal amplification instrumentation developed at our laboratory may be found in Eberstein**. The second method uses a contact on the diaphragm plunger to close a simple trigger circuit which sends a 10 volt signal to the delay unit which in turn triggers the thyratron amplifier and spark source combination. The signal is also sent to a counter (Beckman, Universal EPUT and Timer Model 7360) which is connected to the output of the phototube. In this way, the plunger contact signal is referenced to the phototube output signal so that a consistent timing reference is used.

The still interferograms are recorded by a Leica camera with a f/4.5, 135 mm lens with a close-up bellows set at a magnification ratio of approximately 1.01. The image of the flow is recorded on Kodak Tri-X Pan, 35 mm film with an ASA rating of 400. Shadowgraphs are recorded on 4 x 5 in. type 52 Polaroid film, and in both photographic systems the exposure is determined by the short duration (0.5×10^{-6} sec.) spark source. Shadowgraph movies of the flow in the nozzle are obtained by a Fastax 16 mm Model WF3 high-speed motion picture camera in the framing mode at approximately 5000 frames per second. Streak interferograms were made by using this camera in the streak mode (by removal of rotating prism). The light source in each case is a 100 watt mercury arc lamp driven by a 50 volt d.c. power supply.

---

*Klikoff, W. A. 1965 Propagation of weak conical disturbances in relaxing supersonic flows. D. Eng. Thesis, Yale University, New Haven.

**Eberstein, I. J. 1966 Evaluation of light deflection technique for detection of transient shock waves. Rev. of Sci. Inst. 37, 959.

APPENDIX II

TABULATED RESULTS

Spark Shadowgraph Experiments

Spark shadowgraph pictures of the flow in the M = 1.67 3° - 1/2 angle nozzle without a model present were taken during the starting process using dry air. The initial pressure in the high pressure section (P₄) was 1 atm at 21.1°C. An initial pressure ratio (P₄/P₁) of 7.6 was used. Pictures were taken every .05 msec starting at .29 msec after diaphragm rupture to steady flow. The field of view contained the nozzle throat and 3" downstream. Spark shadowgraph pictures were also taken with the nozzle exit and 2" upstream of the exit in the field of view by moving the nozzle 4 in. upstream. No shock waves were seen during these experiments.

Another set of spark shadowgraph pictures of the nozzle exit where a .625 in. spherical model was placed was taken. The pictures show the formation of the steady state detached shock wave which forms around the front of the model. No starting shocks which pass across the model were seen. In Figure II.1 eight spark shadowgraph pictures of the flow over the spherical model during the starting process are shown. Flow is from left to right. The first picture which was taken at t = 1.85 msec after diaphragm rupture shows the shear layer at the exit of the nozzle. As time progresses, the detached shock is formed and finally reaches its steady state configuration at t = 4.53 msec after diaphragm rupture. The last picture at t = 7.08 msec is included to show that the flow is steady by a comparison with the previous picture.

High Speed Shadowgraph Movies

High speed shadowgraph movies of the flow through the nozzle during the starting process were made by using a Fastax WF-3 high speed 16 mm camera at a framing rate of 5000 frames per second. Either dry air or N₂ at 21.1°C was used in the experiments. The experiments were made with the initial pressure (P₄) in the high pressure tube at 3.04 atm and various pressure ratios (P₄/P₁) between 7.6 and 46. Two different nozzle positions were used in all experiments so that the flow between the nozzle throat and exit could be observed. A similar set of experiments were also made with a .5" spherical model at the nozzle exit. Experiments were performed with the M = 1.67 3° - 1/2 angle nozzle and the M = 3 nozzle. Results of these experiments showed no starting shock waves.

To improve the qualitative aspects of the above experiments the following modifications were made. Three 1/8" x 2" thin tape strips were placed along the lower M = 1.67 nozzle block and perpendicular to the flow. The strips were placed one inch apart starting 1/2" downstream from the throat. These strips produced weak disturbances that could be seen in our shadowgraph pictures during the sonic and supersonic portions of the starting process. This made possible a very accurate measurement of starting times. These experiments showed that supersonic flow can be established very smoothly and without shocks in a nozzle.
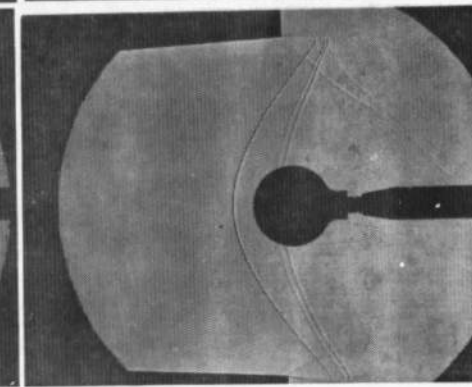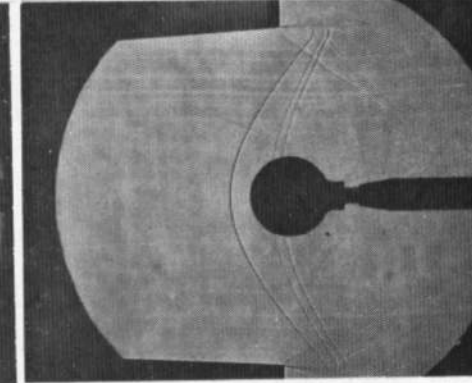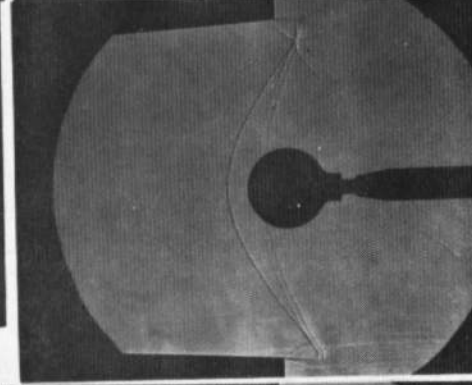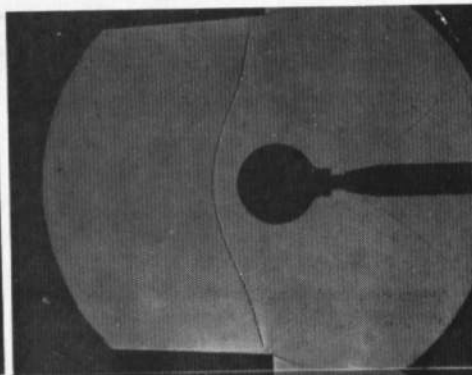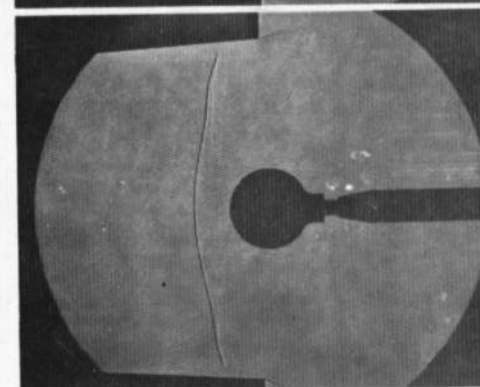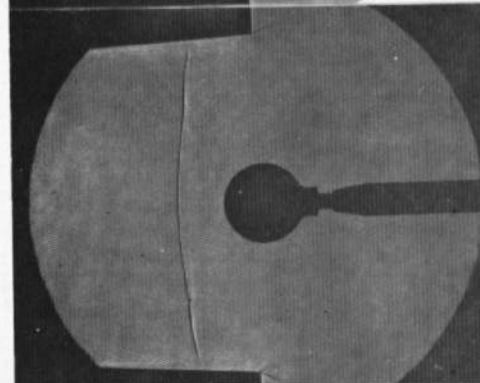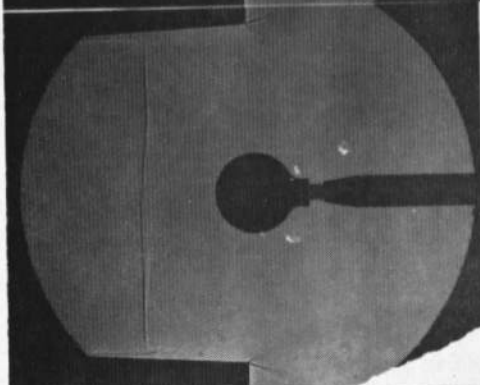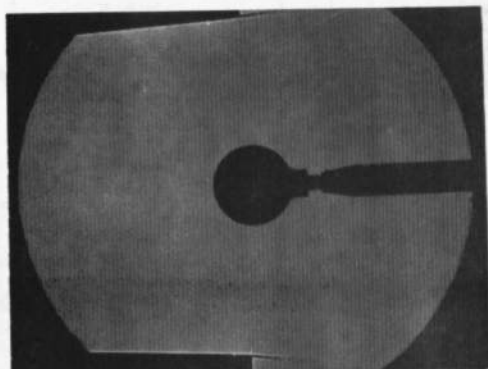
Figure II.1 Time after diaphragm rupture for above shadowgraph pictures are;
(a) 1.85 msec, (b) 2.90 msec, (c) 3.37 msec, (d) 3.51 msec,
(e) 3.80 msec, (f) 4.08 msec, (g) 4.53 msec, (h) 7.08 msec.
Gas: Dry air; Nozzle: M = 1.67. Flow is left to right.

Streak Interferograms

Streak interferograms of the starting process in the M = 1.67 3° - 1/2 angle nozzle and in the M = 3 nozzle were made by using the Fastax WF3 high speed camera in the streak mode. The equivalent film speed was 380 m/sec with a time resolution of approximately 5×10^{-6} seconds. The experiments were performed with dry air or nitrogen at 21.1°C. Various initial pressures (P_4) ranging from 1 atm to 3.3 atm were used together with pressure ratios of 46, 15, and 7.6. Two different nozzle positions were used in all experiments so that interferograms of the flow between the nozzle throat and exit were obtained. The quantitative results of these experiments were density time histories at various positions downstream of the nozzle throat during the starting process. These show that the density undershoots its steady state value during the starting process. It also shows that the undershoot is most pronounced at and near the throat and that it diminishes with increasing downstream distance until finally at the exit it is not present. Density profiles along the nozzle centerline between the throat and exit for a particular time during the starting process are also obtained from these experiments. Since they do not contain any discontinuities in density, no shock waves were detected during the starting process.

Static Pressure Measurements

Static pressure measurements of the supply pressure were made between the exit of the high pressure tube and the transition section. Static pressure measurements of the pressure in the nozzle were also made at three positions in the nozzle; at the nozzle throat, near the exit and just outside the exit. The measurements of the static supply pressure show that the initial pressure (P_4) first undershoots and then slightly overshoots the steady flow supply conditions before it becomes steady. Measurements made in the nozzle show that the undershoot effect is present at the nozzle throat and diminishes with downstream distance until finally at the nozzle exit is is not present, that is, at the exit the pressure decreases monotonically to the steady state static pressure. These experiments were made using N_2 at 21.1°C at initial pressure (P_4) ranging from 1 atm to 3.04 atm with various pressure ratios between 7.6 and 46. In all cases the initial pressure and pressure ratios had no effect on the undershoot.

In Figure II.2, four oscilloscope traces of the static pressure measurements of the supply tube are shown. The gas used in these experiments was dry air at 1 atm and 21.1°C in the supply tube. The pressure in the low pressure tube was varied between .079 atm and .289 atm so that initial pressure ratios (P_4/P_1) between 12.65 and 3.46 could be obtained. The vertical scale is .5 psi/div and the horizontal scale is 2 msec/div for all traces. Results of these experiments show that the undershoot is not effected by the pressure ratio as long as supersonic flow is established in the nozzle. The steady state supply pressure is not effected by boundary layer growth in this tube as can be seen from the pressure traces. The effect of the reflected expansion wave is clearly shown in these pressure traces.

In Figure II.3, three oscilloscope traces of the static pressure measurements of the supply tube are shown. The gas used was dry air at 21.1°C. In the first trace, the initial pressure (P_4) was 3.38 atm and the low pressure

$P_4/P_1 = 12.65$
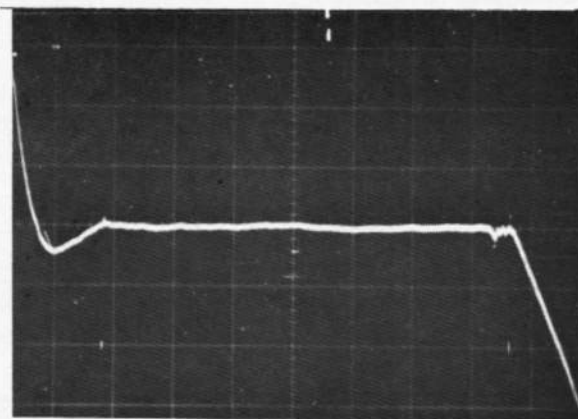
$P_4/P_1 = 5.45$
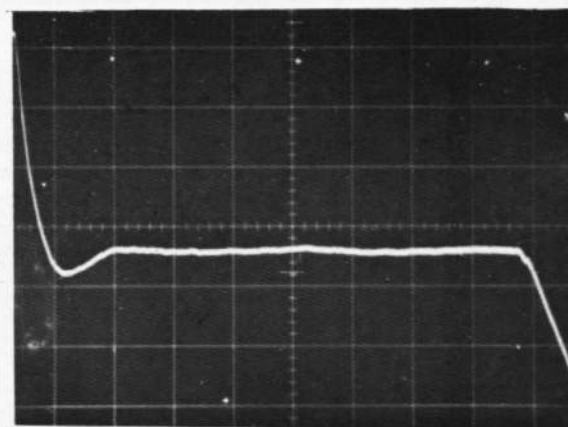
$\Delta P(.5 \text{ psi/div}) \rightarrow$

t(2 msec/div)

$P_4/P_1 = 4.22$
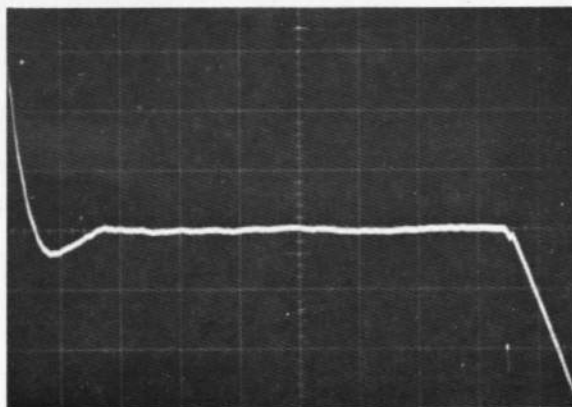
$P_4/P_1 = 3.46$

$\Delta P(.5 \text{ psi/div}) \rightarrow$
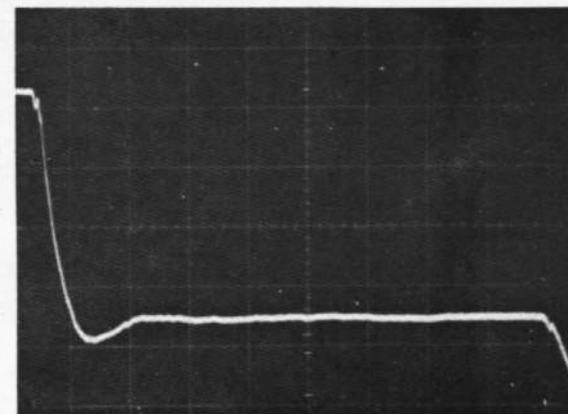
t(2 msec/div) →

Figure II.2 Supply pressure vs. time at upstream position. Initial pressure,
P₄, is 1 atm. while low pressure, P₁, is varied to yield different
pressure ratio. Gas: Dry air; Nozzle: M = 1.67.
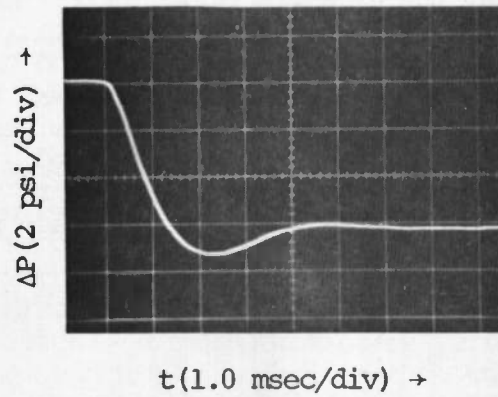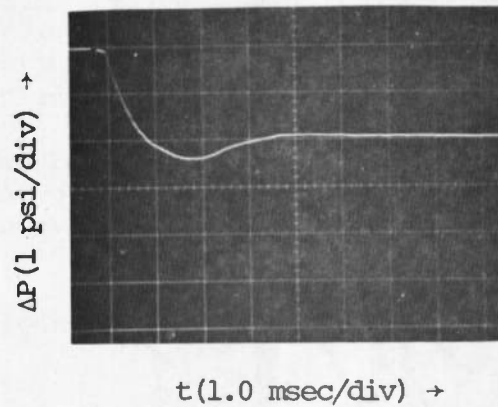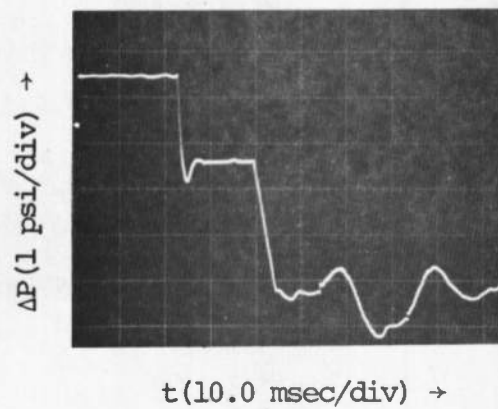
Figure II.3 Supply pressure vs. time at upstream
            position. Gas: Dry air; Nozzle: M = 1.67

27

(P_1) was .131 atm so that the pressure ratio (P_4/P_1) was 25.8. The undershoot again appears and is clearly not a function of initial pressure or pressure ratio as can be seen by comparing it with the second trace which was taken with P_4 = 1 atm and P_4/P_1 = 7.6. The third trace was taken with the gas pressure and pressure ratio the same as in the second picture, but the time scale was changed so that a long time history was recorded. This trace shows the starting of the second steady state period. However, it is interrupted by the reflected shock wave which started when the diaphragm ruptured and reflected off the end plate of the low pressure tube.

APPENDIX III

DETAILS OF NUMERICAL CALCULATIONS

A numerical technique was used to calculate the gas properties in the nozzle during the starting process using the method of characteristics. The following assumptions were made in the analysis; that the gas is inviscid, non-conducting and has constant specific heats and that the flow is adiabatic and one-dimensional with area change. It was also assumed that the flow of the gas in the high pressure tube is initiated by a centered expansion wave at the diaphragm position. This assumption is valid only if the characteristic time for diaphragm rupture is much less than the characteristic time of the nozzle flow which is the time a sound wave takes to travel the length of the nozzle. In this case the time for diaphragm rupture is less than .1 msec and the characteristic time of nozzle flow is 1 msec. The calculations were made using the non-dimensional characteristic equations. A derivation of the characteristic equations and details of the numerical technique are given below.

Derivation of Characteristic Equations

A brief derivation of the characteristic equations follow, however, for a more detailed derivation, see Reference 8. The conservation equations of mass and momentum for one-dimensional flow with area change, $A(x)$, are:

$$\frac{\partial \rho}{\partial t} + u \frac{\partial \rho}{\partial x} + \rho \frac{\partial u}{\partial x} + \rho u \frac{d \ln A}{dx} = 0 \tag{1}$$

$$\frac{\partial u}{\partial t} + u \frac{\partial u}{\partial x} = -\frac{1}{\rho} \frac{\partial p}{\partial x} \tag{2}$$

and the thermal equation of state for a perfect gas is

$$p = \rho RT$$

where u is the particle velocity, ρ the density, A the area, R the gas constant, p the pressure and T the absolute temperature. For the remaining derivation, subscripts will be used to denote partial derivatives.

For isentropic flow,

$$p = p\,(\rho,\, s_o)$$

from which

$$dp = \left(\frac{\partial p}{\partial \rho}\right)_{s_o} d\rho = a^2\,(\rho)\,d\rho \tag{3}$$

where a^2 is defined as the equilibrium sound speed.

Using equation (3), equation (2) becomes,

$$u_t + u\, u_x + \frac{a^2(\rho)}{\rho}\, \rho_x = 0 \tag{3a}$$

By multiplying equation (1) by $\pm \frac{a}{\rho}$ and adding (3a), the following equations are formed,

$$u_t + (u + a)u_x + \frac{a}{\rho}\,[\rho_t + (u + a)\rho_x] = -\,ua\,(\ell n\ A)_x \tag{4}$$

$$u_t + (u - a)u_x - \frac{a}{\rho}\,[\rho_t + (u - a)\rho_x] = ua\,(\ell n\ A)_x \tag{5}$$

Two characteristic curves are defined by specifying their slopes. A right running characteristic curve, C_{rr} , is defined as a curve in the $x - t$ plane with a slope equal to $dx/dt = u + a$ and a left running characteristic curve, $C_{\ell r}$, is defined as a curve in the $x - t$ plane with a slope equal to $dx/dt = u - a$. A change in any quantity, ϕ , along C_{rr} or $C_{\ell r}$ is written as

$$d\phi = [\phi_t + (u \pm a)\phi_x]dt$$

A new variable, $w(\rho)$, is defined by

$$w(\rho) = \int_{\rho_o}^{\rho} \frac{a(\rho)}{\rho}\, d\rho$$

when $dw = \frac{a}{\rho}\, d\rho$. For a gas with constant specific heats this becomes,

$$w(\rho) = \frac{2}{\gamma - 1}\, a_o \left[\left(\frac{\rho}{\rho_o}\right)^{\frac{\gamma - 1}{2}} - 1\right]$$

or

$$w(a) = \frac{2}{\gamma - 1}\,(a - a_o)$$

Substituting this into equations (4) and (5) and multiplying each by dt, one has,

$$[u_t + (u + a)u_x]dt + [w_t + (u + a)w_x]dt = -ua \; (\ell n \; A)_x \; dt$$

$$[u_t + (u - a)u_x]dt - [w_t + (u - a)w_x]dt = ua \; (\ell n \; A)_x \; dt$$

By denoting changes along a characteristic with a delta, δ, the above equations are rewritten as,

$$\delta_r \; (u + w) = -ua \; (\ell n \; A)_x \; dt \tag{6}$$

$$\delta_\ell \; (u - w) = ua \; (\ell n \; A)_x \; dt \tag{7}$$

where the subscripts "r" and "ℓ" refer to the right and left characteristic curves. The equations are the governing characteristic equations for isentropic one-dimensional flow with area change.

Equations (6) and (7) can be rewritten in non-dimensional form by using a_0 as a characteristic velocity, which is the initial sound speed of the gas in the high pressure tube, L as a characteristic length which in this case will be the nozzle length, and L/a_0 as a characteristic time. The following non-dimensional variables are thus defined.

$$\bar{A} = \frac{a}{a_0}$$

$$U = \frac{u}{a_0}$$

$$W = \frac{w}{a_0}$$

$$z = \frac{x}{L}$$

$$\tau = \frac{t}{L/a_0}$$

Substituting the above into equations (6) and (7) the non-dimensional equations follow:

$$\delta_r \; (U + W) = -U\bar{A} \; (\ell n \; A)_z \; d\tau \tag{8}$$

$$\delta_\ell \; (U - W) = U\bar{A} \; (\ell n \; A)_z \; d\tau \tag{9}$$

31

The non-dimensional equations for the characteristic curves are:

$$C_{rr}: \quad \frac{dz}{d\tau} = U + \bar{A}$$

$$C_{\ell r}: \quad \frac{dz}{d\tau} = U - \bar{A}$$

Equations (8) through (11) and the appropriate boundary conditions are all that is necessary for a numerical solution.

Numerical Technique

The numerical technique uses the properties of a centered expansion wave and the initial known conditions to calculate the coordinates of each left running characteristic in the centered expansion wave which travels into the nozzle and also the gas properties at each coordinate. The coordinates of a point on a characteristic curve are determined by the intersection of a right and left characteristic curve each starting from two different but nearby points when the properties of the gas are known. It is assumed that the slopes of the right and left characteristic curves do not change significantly between the known points and the points of intersection. This assumption is justified if the points are very near each other. Since the characteristic equations relate the change in (U + W) and (U - W) along a left and right characteristic curve for changes in τ , they may be written in difference form to approximate changes in (U + W) and (U - W) for small $\Delta\tau$. This method is used to calculate the properties of the gas at the intersection point of the left and right characteristics which start from two different known points. The two resulting equations are solved for U and W and hence all the properties of the gas at that point are known. This process is repeated until all the coordinates of a particular left characteristic and the gas properties along it are known. The next characteristic in the centered expansion fan is then calculated in a similar manner by starting at the beginning of the characteristic and using the calculated results along the previous characteristic.

The details of the calculation follow. In Figure III.1 a $z - \tau$ diagram is shown with the first left running characteristic drawn. It is a straight line because the first left running characteristic of the centered expansion fan is moving into a gas which is at rest and therefore moves with a constant velocity equal to $- \bar{A}_0$. Along this characteristic all the properties of the gas are known; they are the initial conditions of the gas. Therefore, at any point along this characteristic the slope of a right running characteristic starting at that point is known and is A_0 . In particular, all the properties at point 2 are known. Since the flow is started by a centered expansion wave at $z = 0$ and $\tau = 0$, all the properties of the gas are known at point 1 for a given left running characteristic starting at this point with a known slope. This can be shown by noting the relation that exists through a simple expansion fan for the velocity and sound speed as related to the initial sound speed. This relation is
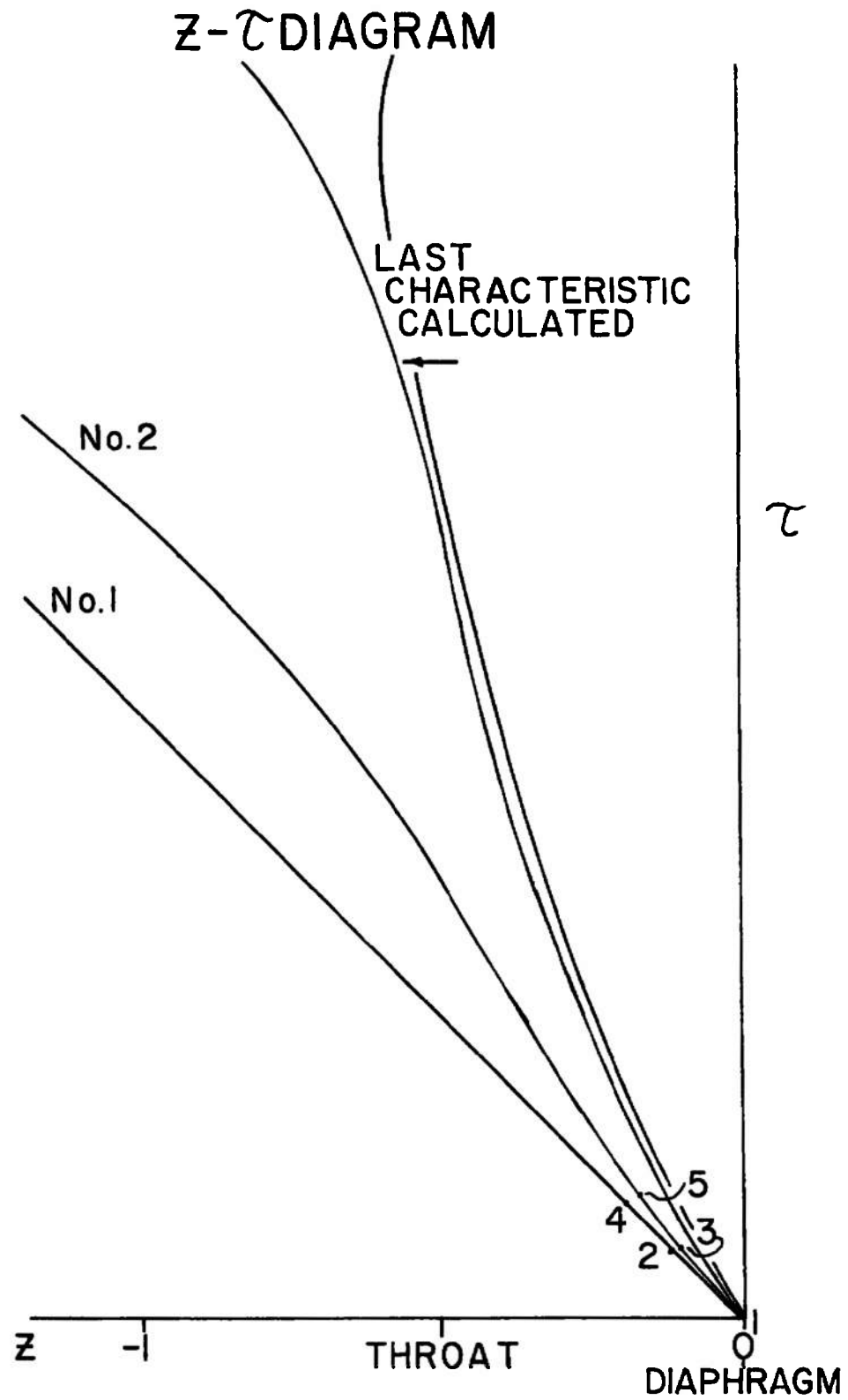
Figure III.1

$$U + \frac{2}{\gamma - 1} \bar{A} = \frac{2}{\gamma - 1} \bar{A}_O$$

The slope of the left running characteristic in the expansion fan is,

$$SL = U - \bar{A}$$

From the above equation, U and $\bar{A}$ can be written in terms of the initial slope, SL, as follows,

$$\bar{A} = \frac{\gamma - 1}{\gamma + 1} \left[\frac{2}{\gamma - 1} - SL \right]$$

$$U = SL + \bar{A}$$

$$W = \frac{2}{\gamma - 1} \bar{A}$$

Therefore, by specifying the initial slope of the left running characteristic which starts at point 1 all the properties of the gas at this point are known.

Since the coordinates of both points 1 and 2 and the slope of the respective left and right running characteristic are known, the intersection of the two characteristics can be found and therefore the coordinates of that point. Next, to find the properties of the gas at point 3 the characteristic equations are written in difference form in the following way:

along C_{rr}

$$(U + W)_3 - (U + W)_2 = - (U\bar{A})_2 \left(\frac{1}{A} \frac{dA}{dz} \right)_2 (\tau_3 - \tau_2)$$

along $C_{\ell r}$

$$(U - W)_3 - (U - W)_1 = (U\bar{A})_1 \left(\frac{1}{A} \frac{dA}{dz} \right)_1 (\tau_3 - \tau_1)$$

The above equations are then solved for W_3 and U_3 and thus all the properties of the gas are known for point 3. The same procedure is used to find the coordinates of the next point on the No. 2 left characteristic and then all the gas properties at that point. This is continued until all the coordinates and gas properties along this characteristic have been calculated. Then the No. 3 left characteristic is calculated using the same procedure but in this case using the calculated properties along No. 2 left characteristic and point 1 for the initial angle of the new characteristic.

For the above calculations the initial $\Delta\tau$ used for calculation of No. 2

34

left characteristic was of the order of .01 and thereafter was determined by the intersection of the characteristics. The initial slope of all left characteristics starting at point 1 differed from the previous one by .001 degrees.

Computer Technique and Program Flow Chart

The computer technique consisted of three basic phases, input, calculations and output. The input phase reads in all pertinent data on the gas, such as, specific heat, initial velocity, and sound speed, initial increments in $\Delta \tau$ and change in characteristic initial angles, the nozzle area as a function of z, and frequency of output printouts. The calculations were performed for one characteristic at a time. After all data for a new characteristic was computed it was printed by the computer printer and then used as the known characteristic for the next calculation. The output phase printed the coordinates of each new characteristic together with the correspoinding gas velocity, sound speed and Mach numbers at that point. The slope of the right and left running characteristic was also printed out for each coordinate. By selection of the appropriate control variables, only predetermined characteristics were printed. A simple flow chart of the program is shown in Figure III.2.

A problem which prevented a complete solution to the starting process was encountered. This problem is basically due to the divergence of the left characteristics near and at the nozzle throat when the Mach number approaches one. When this happens the assumption that the intersection of the right and left running characteristic is near the starting point of the two characteristics is invalid. Therefore, the increments must be decreased in size continuously to maintain the validity of the above assumption. At this time only the results of the program where the assumptions are valid are used. Figure III.1 shows the divergence of the characteristics at and near the nozzle throat as Mach 1 is approached.
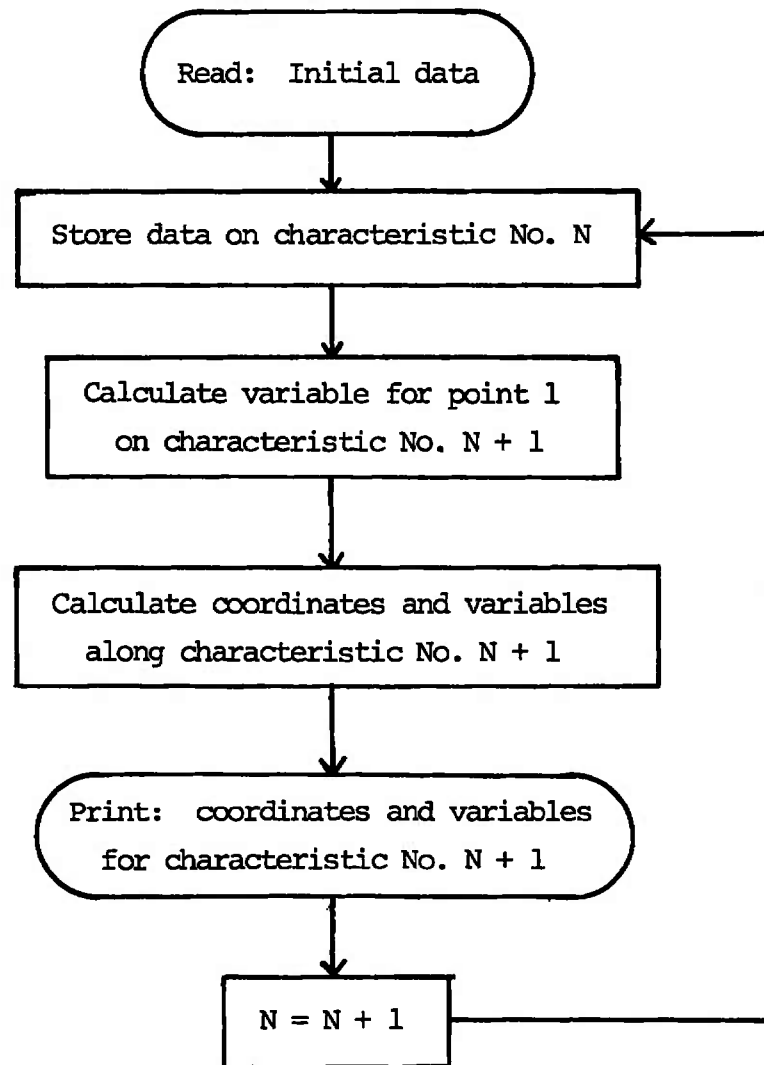
35

Simplified Flow Chart

Figure III.2

REFERENCES

1. Davis, John W. 1968 "A Shock Tube Technique for Producing Subsonic, Transonic and Supersonic Flows with Extremely High Reynolds Numbers". Paper 68-18, AIAA.

2. Ludwieg, H. 1955 "Der Rohrwindkanal". Zeitschrift für Flugwissenschaft, Jahrgang 3, Heft 7, 206; see also Ludwieg, H., "Tube Wind Tunnel: A Special Type of Blowdown Tunnel". NATO Advisory Group for Aeronautical Research and Development Report 143, July, 1957.

3. Wegener, P. P., and Buzyna, G. 1969 "Experiments on Shock Stand-off Distance in Non-equilibrium Flow". J. Fluid Mech., 37, 325.

4. Cable, A. J., and Cox, R. N. 1963 "The Ludwieg Pressure-Tube Supersonic Wind Tunnel". The Aeronautical Quarterly.

5. Becker, E. 1957 Grenzschichteffekte beim Rohrwindkanal. WGL-Tagung Essen.

6. Johnson, Joseph A. III and Cagliostro, D. 1969 "Gasdynamic Starting Processes in a Supersonic Ludwieg Tube". Bull. Am. Phys. Soc., 14, 527.

7. Hottner, Th. 1965 "Untersuchungen an einem Modell-Rohrwindkanal für Machzahlen von M = 3 bis 6". Zeitschr. für Flugwissen., 13, 237.

8. Rudinger, G. 1969 "Nonsteady Duct Flow: Wave Diagram Analysis". Dover Publications, Inc., New York.

DOCUMENT CONTROL DATA - R & D

(Security classification of title, body of abstract and indexing annotation must be entered when the overall report is classified)

1. ORIGINATING ACTIVITY *(Corporate author)*	2a. REPORT SECURITY CLASSIFICATION
Yale University, Department of Engineering and Applied Science, New Haven, Conn. 06520	UNCLASSIFIED
	2b. GROUP N/A

3. REPORT TITLE

EXPERIMENTS WITH A SUPERSONIC TUBE WIND-TUNNEL

4. DESCRIPTIVE NOTES *(Type of report and inclusive dates)*
October 1968 to November 1969 - Final Report

5. AUTHOR(S) *(First name, middle initial, last name)*

Joseph A. Johnson, III and Dominic Cagliostro, Yale University

6. REPORT DATE	7a. TOTAL NO. OF PAGES	7b. NO. OF REFS
March 1970	48	8

8a. CONTRACT OR GRANT NO. AF 40(600)-1133	9a. ORIGINATOR'S REPORT NUMBER(S)
b. Program Element 62201F	AEDC-TR-70-71
c. Project 8952	9b. OTHER REPORT NO(S) *(Any other numbers that may be assigned this report)*
d. Task 08	N/A

10. DISTRIBUTION STATEMENT

This document has been approved for public release and sale; its distribution is unlimited.

11. SUPPLEMENTARY NOTES	12. SPONSORING MILITARY ACTIVITY
Available in DDC.	Arnold Engineering Development Center (AEDC), AFSC, Arnold Air Force Station, Tennessee 37389

13. ABSTRACT

An experimental study has been performed of the unsteady processes in the starting period of a supersonic Ludwieg tube, a device which operates like an intermittent supersonic wind tunnel. A quick opening diaphragm located downstream of the nozzle initiates the flow. Pressure and density measurements are made in a variety of ways in Mach number 1.67 and 3.0 nozzles. For the starting conditions treated, supersonic flow is established in the nozzle without producing shock waves. Various time dependent functions are observed in the adjustment of gasdynamic parameters to their steady supersonic values. These changes of pressure, etc., include undershoots, overshoots, and other variations of the final steady-state values. Calculations based on an assumed zero-length nozzle do not adequately predict starting times and pressures.

DD FORM 1473
1 NOV 65

14. KEY WORDS	LINK A		LINK B		LINK C	
	ROLE	WT	ROLE	WT	ROLE	WT
supersonic wind tunnels						
aerodynamics						
supersonic flow						
experimentation						
density measurement						
pressure measurement						

AFSC
Arnold AFS Tenn